

# Causes and consequences of pronounced variation in the isotope composition of plant xylem water

Hannes P.T. De Deurwaerder<sup>1,2</sup>, Marco D. Visser<sup>2</sup>, Matteo Detto<sup>2</sup>, Pascal Boeckx<sup>3</sup>, Félicien Meunier<sup>1,4</sup>, Kathrin Kuehnhammer<sup>5,6</sup>, Ruth-Kristina Magh<sup>7,8</sup>, John D. Marshall<sup>8</sup>, Lixin Wang<sup>9</sup>, Liangju Zhao<sup>10,11</sup>, Hans Verbeeck<sup>1</sup>

<sup>1</sup> CAVELab - Computational & Applied Vegetation Ecology, Faculty of Bioscience Engineering, Ghent University, Ghent, Belgium

<sup>2</sup> Department of Ecology and Evolutionary Biology, Princeton University, Princeton, NJ, USA

<sup>3</sup> ISOFYS – Isotope Bioscience Laboratory, Faculty of Bioscience Engineering, Ghent University, Ghent, Belgium

<sup>4</sup> Ecological Forecasting Lab, Department of Earth and Environment, Boston University, Boston, Massachusetts, USA

<sup>5</sup> IGOE, Umweltgeochemie, Technische Universität Braunschweig, Braunschweig, Germany

<sup>6</sup> Ecosystem Physiology, University of Freiburg, Freiburg, Germany

<sup>7</sup> Institute for Forest Sciences, Chair of Tree Physiology, University of Freiburg, Freiburg, Germany

<sup>8</sup> Department of Forest Ecology and Management, SLU, Swedish University of Agricultural Sciences, Umeå, Sweden

<sup>9</sup> Department of Earth Sciences, Indiana University-Purdue University Indianapolis (IUPUI), Indianapolis, IN 46202, USA

<sup>10</sup> Shaanxi Key Laboratory of Earth Surface System and Environmental Carrying Capacity, College of Urban and Environmental Sciences, Northwest University, Xi'an 710127, China

<sup>11</sup> Key Laboratory of Ecohydrology and Integrated River Basin Science, Northwest Institute of Eco-Environment and Resources, Chinese Academy of Sciences, Lanzhou 730000, China

*Correspondence to:* Hannes P.T. De Deurwaerder (Hannes\_de\_deurwaerder@hotmail.com)

## Abstract

1. Stable isotopologues of water are widely used to derive relative root water uptake (RWU) profiles and average RWU depth in lignified plants. Uniform isotope composition of plant xylem water ( $\delta_{xyl}$ ) along the stem length of woody plants is a central assumption of the isotope tracing approach, which has never been properly evaluated.
2. Here we evaluate whether strong variation in  $\delta_{xyl}$  within woody plants exists using empirical field observations from French Guiana, northwestern China, and Germany. In addition, supported by a mechanistic plant hydraulic model, we test hypotheses on how variation in  $\delta_{xyl}$  can develop through the effects of diurnal variation in RWU, sap flux density, diffusion, and various other soil and plant parameters on the  $\delta_{xyl}$  of woody plants.
3. The hydrogen and oxygen isotope composition of plant xylem water shows strong temporal (i.e., sub-daily) and spatial (i.e., along the stem) variation ranging up to 25.2‰ and 6.8‰ for  $\delta^2\text{H}$  and  $\delta^{18}\text{O}$  respectively, greatly exceeding measurement error range in all evaluated datasets. Model explorations predict that significant  $\delta_{xyl}$  variation could arise from diurnal RWU fluctuations and vertical soil water heterogeneity. Moreover, significant differences in  $\delta_{xyl}$  emerge between individuals that differ only in sap flux densities, or are monitored at different times or heights.
4. This work shows a complex pattern of  $\delta_{xyl}$  transport in the soil-root-xyle system, which can be related to the dynamics of RWU by plants. These dynamics complicate the assessment of RWU when using stable water isotopologues, but also open new opportunities to study drought responses to environmental drivers. We propose to include monitoring of sap flow and soil matric potential for more robust estimates of average RWU depth and expansion of attainable insights in plant drought strategies and responses.

## Keywords

Ecohydrology, Lianas, Root water uptake, Sap flow, Stable isotope composition of water, Tropical trees, Water competition

## 1. Introduction

The use of stable isotope composition of water has strengthened ecohydrology studies by providing insights into phenomena that are otherwise challenging to observe, such as relative root water uptake depth (RWU depth) (Rothfuss & Javaux, 2017), below-ground water competition and hydraulic lift (Hervé-Fernández *et al.*, 2016; Meunier *et al.*, 2017). Compared to root excavation, the technique is far less destructive and labor-intensive. This makes it more flexible for studying multiple individuals across spatial and temporal scales (i.e. individual to ecosystem, daily to seasonal) (Dawson *et al.* 2002). Besides, the study of stable isotope composition of xylem water measures the real effects of RWU at different depths whereas excavation yields only root distribution and architecture. The advantages and wide applicability of this method make it a popular technique that pushes the boundaries of ecohydrology (Dawson *et al.*, 2002; Yang *et al.*, 2010; Rothfuss & Javaux, 2017; Lanning *et al.*, 2020)

A variety of methods are used to infer average RWU depth from the isotope composition of plant xylem water ( $\delta_{\text{xyl}}$ ), but all rely on a direct relationship between the isotopic compositions of plant xylem and soil water (Ehleringer & Dawson, 1992). All have two key assumptions. The first is that the isotope composition of plant xylem water remains unchanged during transport from root uptake to evaporative sites (e.g. leaves and non-lignified green branches). Hence, isotopic fractionation – i.e. processes that cause a shift in the relative abundances of the water isotopologues, driven by their differences in molecular mass – do not occur during the transport from the uptake to the evaporative site (Wershaw *et al.*, 1966; Zimmermann *et al.*, 1967; White *et al.*, 1985; Dawson & Ehleringer, 1991; Walker & Richardson, 1991; Dawson *et al.*, 2002; Zhao *et al.*, 2016). Second, all methods assume that xylem water provides a well-mixed isotope composition of water from different soil layers: sampled xylem water instantaneously reflects the distribution and water uptake of the roots independent of the timing or height of sampling.

The first assumption is relatively well supported. Isotopic fractionation at root level does not raise concerns for most RWU assessments using water isotopologues (Rothfuss & Javaux, 2017) except for kinetic fractionation that might occur during water transported across the root membrane in extreme environments (Lin & Sternberg, 1993; Ellsworth and Williams, 2007; Zhao *et al.*, 2016). Similarly, isotopic fractionation of water within an individual plant, although possible, is generally not considered a serious problem (Yakir, 1992; Dawson & Ehleringer, 1993; Cernusak *et al.*, 2005; Mamonov *et al.*, 2007; Zhao *et al.*, 2016). This perception was recently contested by Barbeta *et al* (2020), advocating a more general nature of the occurrence of isotopic offsets between xylem water and potential water sources. As the origin of these offsets remains debated, future research should clarify its impact on the applicability of stable water isotopic compositions for RWU assessment. However, the second assumption of time and space invariance of the isotope composition of xylem water has, to our knowledge, never been assessed.

Various plant physiological processes, ranging from very simple to more complex mechanisms, could influence within plant variation in  $\delta_{\text{xyl}}$  at short time scales, i.e. sub-daily to sub-hourly. For instance, plant transpiration during the day is regulated by stomata according to water supply and atmospheric demand, and follows well known diurnal patterns (Steppe & Lemeur, 2004; Epila *et al.*, 2017). This results in a changing water potential gradient between soil and leaves throughout the day (Fig 1a,b), which in turn affects the depth of the average RWU (Goldstein *et al.*, 1998; Doussan *et al.*, 2006; Huang *et al.*, 2017). Hence, shifts in a plant's capacity to take up water at different soil layers during the day can generate diurnal variation in the mixture of isotope composition

from water taken up from various depths (Fig 1c). Subsequently, this water mixture moves up along the xylem with the velocity of the sap flux density. As these sap flux densities depend on species and individual-specific hydraulic traits and their responses to atmospheric water demand and soil moisture availability, complex dynamics in isotopic composition will emerge and propagate through the plant. The above hypothesis, if true, would make the comparison of isotopic data among individuals, species, and studies difficult.

In this study, we provide a critical assessment of the assumption of  $\delta_{xyl}$  invariance along the length of woody plant stems and over short time periods. We first show that variation in  $\delta_{xyl}$  along the length of lignified plants exceeds the expected measurement error using three independent datasets including i) canopy trees and lianas sampled at different heights in French Guiana; and ii) plant species from northwestern China (Zhao *et al.*, 2014) and iii) European Beech and Silver firs in south-west Germany (Magh *et al.*, 2020). Second, we build a simple mechanistic model that incorporates basic plant hydraulic transport processes. The model predicts that diurnal changes in water potential gradient between soil and roots result in shifting sources of water absorption that differ in their isotope composition.

## 2. Materials and Methods

### 2.1. Part A: Empirical exploration

#### 2.1.1. Field data French Guiana: variation in $\delta_{xyl}$ with plant height

Six canopy trees and six canopy lianas were sampled during two subsequent dry days (24-25 August 2017) at the Laussat Conservation Area in Northwestern French Guiana (05°28.604'N-053°34.250'W). Stem xylem tissue of individual plants was sampled at different heights (1.3, 5, 10, 15 and 20 m where possible) at the same radial position of the stem, between 9:00 and 15:00. Stem samples were stripped off bark and phloem tissues. Soil samples were collected at different depths (0.05, 0.15, 0.30, 0.45, 0.60, 0.90, 1.20, and 1.80m) with a soil auger and in close vicinity to the sampled individuals. Samples were placed in glass collection vials, sealed with a cap, and frozen awaiting cryogenic vacuum distillation (CVD; 4 h at 105°C). When the weight loss of a sample resulting from the extraction process was below 98%, the sample was excluded (after Araguás-Araguás *et al.*, 1998) (see Fig S1).

The isotope composition of the water in the samples was measured with a Wavelength-Scanned-Cavity Ring-Down Spectrometer (WS-CRDS, L2120-i, Picarro, California, USA) coupled with a vaporizing module (A0211 High Precision Vaporizer) and a micro combustion module to avoid organic contamination (Martin-Gomez *et al.*, 2015; Evaristo *et al.*, 2016). Post-processing of raw  $\delta$ -readings into calibrated  $\delta$ -values (in ‰, V-SMOW) was performed using SICalib (version 2.16; Gröning, 2011). More details on the sampling site and sampling procedure can be found in supplementary methods A.

#### 2.1.2. Field data China: temporal variation in $\delta_{xyl}$

Plant  $\delta_{xyl}$  was sampled at high temporal resolution in the Heihe River Basin (HRB), northwestern China. Four distinct study locations differing in altitude, climatological conditions, and ecosystem types were selected. At each location, the dominant tree, shrub, and/or herb species were considered for sampling. In August 2009, *Populus euphratica* was sampled in the Qidaoqiao riparian forest (42°01'N-101°14'E) and *Reaumuria soongorica* in the

Gobi desert ecosystem (42°16'N-101°17'E; 906-930 m a.s.l.). In June–September 2011 *Picea crassifolia*, *Potentilla fruticosa*, *Polygonum viviparum* and *Stipa capillata* were measured in the Pailugou forest ecosystem (38°33'N-100°18'E; 2700-2900 m a.s.l.). All species were sampled every 2-hours over multiple days (3-4), except for *P. crassifolia*, which was measured hourly. Stem samples were collected for trees and shrubs, while root samples were obtained for the herb species. More details are available in Zhao *et al.* (2014).

Upon collection, all samples were placed in 8 mL collection bottles and frozen in the field stations before transportation to the laboratory for water extraction via CVD (Zhao *et al.*, 2011). Both  $\delta^{18}O$  and  $\delta^2H$  were assessed with an Euro EA3000 element analyzer (Eurovector, Milan, Italy) coupled to an Isoprime isotope ratio mass spectrometer (Isoprime Ltd, UK) at the Heihe Key Laboratory of Ecohydrology and River Basin Science, Cold and Arid Regions Environmental and Engineering Research Institute. Internal laboratory references were used for calibration, resulting in measurement precision of  $\pm 0.2\%$  and  $\pm 1.0\%$  for  $\delta^{18}O$  and  $\delta^2H$ , respectively.

### 2.1.3. Field data Germany: high temporal variation in $\delta_{xyl}$

A  $\delta_{xyl}$  monitoring campaign, studying mature Silver firs (*Abies alba*; n=3) and European beeches (*Fagus sylvatica*; n=3), was conducted during progressing drought conditions (6-11 July 2017) at the “Freiamt” field site in south-west Germany. Isotopic composition of xylem water was obtained from branch samples, which were collected every two hours between 7:00 and 21:00 at the same height and canopy orientation in the sun crown. Branches were stripped of bark and phloem tissue. A Scholander Pressure chamber (Scholander, 1966), which allowed concomitant registration of water potential of the sampled branches, was used to extract xylem water directly in the field (Rennenberg *et al.*, 1996). Both  $\delta^{18}O$  and  $\delta^2H$  of branch samples were determined with a wavelength scanned cavity ring-down spectrometer (Picarro L2130i, Santa Clara, USA), followed by data correction using ChemCorrect™ (Picarro, 2010). For more details see Magh *et al.* (2020).

### 2.1.4. Field data normalization

To aid visual comparisons, we use normalized  $\delta_{xyl}$  values ( $\beta^2H_X$  and  $\beta^{18}O_X$ ) which describe the deviation of an individual sample from the average isotopic composition (a) along the height  $h$  of the stem, or (b) over one day:

$$\beta^2H_X = \delta^2H_X - \frac{1}{N} \sum_{j=1}^N \delta^2H_{X,j} \quad (1)$$

With  $N$  the number of sampled heights or time steps during one day.

## 2.2. Part B: Model exploration

### 2.2.1. Model derivation

The expected  $\delta_{xyl}$  at different stem heights within a tree during the course of the day can be derived from plant and physical properties such as root length density, total fine root surface area, water potential gradients, and the isotope composition of soil water (Fig. 2). We call this the SWIFT model (i.e. Stable Water Isotopic Fluctuation within Trees). To derive the SWIFT model, we first describe the establishment of  $\delta_{xyl}$  entering the tree at the stem base via a multi-source mixing model (Phillips & Gregg, 2003). We subsequently consider vertical water transport within the tree, which relates to the established sap flow pattern.

To ensure consistency and clarity in variable declarations we maintain the following notation in the subscripts of variables: uppercase roman to distinguish the medium through which water travels (X for xylem, R for root, S for soil) and lowercase for units of time and distance ( $h$  for stem height,  $t$  for time and  $i$  for soil layer index). A comprehensive list of variables, definitions, and units is given in Table 1. A schematic representation of the model is provided in Fig. 2a. Note that the model presented here focuses on hydrogen isotopes (i.e.  $^2\text{H}/^1\text{H}$ ) but can easily be used to study oxygen isotopes (i.e.  $^{18}\text{O}/^{16}\text{O}$ ).

*i. Isotope composition of plant xylem water at stem base.*

The  $\delta^2\text{H}$  composition of xylem water of an individual plant at stem base ( $\delta^2H_{X,0,t}$ ) (i.e. height zero;  $h = 0\text{m}$ ; Fig. 2a) at time  $t$ , can theoretically be derived by calculating a weighted average of water taken up from different soil depths (Phillips & Gregg, 2003). The root zone is divided into  $n$  discrete soil layers of equivalent thickness  $\Delta z$ . Here, we assume a constant  $\delta^2\text{H}$  composition of soil water ( $\delta^2H_{S,i}$ ) over time in each soil layer, a reasonable assumption when isotopic measurements are conducted during rain-free periods, allowing the expression of  $\delta^2H_{X,0,t}$  as:

$$\delta^2H_{X,0,t} = \sum_{i=1}^n f_{i,t} \cdot \delta^2H_{S,i} \quad (2)$$

where  $f_{i,t}$  is the fraction of water taken up at the  $i^{\text{th}}$  soil layer (Fig. 2a) defined as:

$$f_{i,t} = \frac{RWU_{i,t}}{\sum_{i=1}^n RWU_{i,t}} \quad (3)$$

and  $RWU_{i,t}$  is the net amount of water entering and leaving the roots at time  $t$  in the  $i^{\text{th}}$  soil layer ( $RWU_{i,t}$  is defined positive when entering the root). The current representation of the model does not account for water loss via the root system nor for mixing of the extracted water from different soil layers within the roots until the water enters the stem base. When tree capacitance is neglected, the sum of  $RWU_{i,t}$  across the entire root zone is equal to the instantaneous sap flow at time  $t$ ,  $SF_t$ :

$$SF_t = \sum_{i=1}^n RWU_{i,t} = \sum_{i=1}^n -k_i \cdot A_{R,i} \cdot [\Psi_{X,0,t} - (\Psi_{S,i,t} - z_i)] \quad (4)$$

Where  $k_i$  is the plant-specific total soil-to-root conductance over soil layer  $i$ ,  $\Psi_{X,0,t}$  is the water potential (i.e. the hydraulic head) at the base of the plant stem and  $\Psi_{S,i,t}$  is the soil matric potential at the  $i^{\text{th}}$  soil layer (Fig. 2a). Total plant water potential is generally defined as the sum of the solute, pressure, gravity, and matric potential. As long-distance water transport through the xylem is studied, the osmotic potential and the kinetic energy head can be assumed negligible (Früh & Kurth, 1999). The xylem pressure potential is represented as  $\Psi_{X,0,t}$ . And the term  $z_i$  is the gravimetric water potential necessary to lift the water from depth  $z_i$  to the base of the stem, assuming a hydrostatic gradient in the transporting roots. The model considers  $z_i$  to be a positive value (zero at the surface), thus  $z_i$  is subtracted  $\Psi_{S,i,t}$ .  $A_{R,i}$  is the absorptive root area distribution over soil layer  $i$  (Fig. 2a). This parameter  $A_{R,i}$  can be derived from plant allometric relations with stem diameter (Čermák *et al.*, 2006), and subsequently distributed over the different soil layers, considering the power-law distribution of Jackson *et al.* (1995).

The total soil-to-root conductance is calculated assuming the root and soil resistances are connected in series (Fig. 2a):

$$k_i = \frac{k_R \cdot k_S}{k_R + k_S} \quad (5)$$

where  $k_R$  is the effective root radial conductivity (assumed constant and uniform), and  $k_S = K_{S,i}/\ell$  is the conductance associated with the radial water flow between soil and root surface.  $\ell = 0.53/\sqrt{\pi \cdot B_i}$  represents the effective radial pathway length of water flow between bulk soil and root surface (De Jong van Lier *et al.*, 2008; Vogel *et al.*, 2013) with  $B_i$  giving the overall root length density distribution per unit of soil.  $K_{S,i}$  is the soil hydraulic conductivity for each soil depth.  $K_{S,i}$  depends on soil water moisture and thus relates to the soil matric potential  $\Psi_{S,i,t}$  of the soil layer where the water is extracted.  $K_{S,i}$  is computed using the Clapp & Hornberger (1978) formulation:

$$K_{S,i} = K_{s,max} \cdot \left( \frac{\Psi_{sat}}{\Psi_{S,i,t}} \right)^{2+\frac{3}{b}} \quad (6)$$

where  $K_{s,max}$  is the soil conductivity at saturation and  $b$  and  $\Psi_{sat}$  are empirical constants that depend on soil type (here considered as constant over all soil layers).

Subsequently,  $f_{i,t}$  can be restructured as:

$$f_{i,t} = \frac{k_i \cdot A_{R,i} \cdot \Delta\Psi_{i,t}}{\sum_{i=1}^n k_i \cdot A_{R,i} \cdot \Delta\Psi_{i,t}} \quad (7)$$

where the root water to soil matric potential gradient is represented as  $\Delta\Psi_{i,t} = \Psi_{X,0,t} - (\Psi_{S,i,t} - z_i)$ .

Combining Eq. (2) and Eq. (7) then allows the derivation of  $\delta^2 H_{X,0,t}$  as follows:

$$\delta^2 H_{X,0,t} = \sum_{i=1}^n \left( \frac{k_i \cdot A_{R,i} \cdot \Delta\Psi_{i,t}}{\sum_{j=1}^n k_j \cdot A_{R,j} \cdot \Delta\Psi_{j,t}} \cdot \delta^2 H_{S,i} \right) \quad (8)$$

This equation requires estimates of  $\Delta\Psi_{i,t}$ , which is preferably measured instantaneously in the field (i.e. via stem and soil psychrometers for  $\Psi_{X,0,t}$  and  $\Psi_{S,i,t}$ , respectively). However, as measurements of  $\Psi_{X,0,t}$  are not always available, estimated  $\hat{\Psi}_{X,0,t}$  can be derived from sap flow by re-organizing Eq. (4) into:

$$\hat{\Psi}_{X,0,t} = \frac{\sum_{i=1}^n [k_i \cdot A_{R,i} \cdot (\Psi_{S,i,t} - z_i)] - SF_t}{\sum_{i=1}^n k_i \cdot A_{R,i}} \quad (9)$$

which then allows replacement of  $\Psi_{X,0,t}$  with  $\hat{\Psi}_{X,0,t}$  in Eq. (8).

## ii. Height-dependent isotope composition of plant xylem water

In our model, the water isotopologues simply move upwards from the stem base with the sap flow velocity. Assuming negligible diffusion, the  $\delta^2 H$  isotope composition in xylem water at height  $h$  and time  $t$  ( $\delta^2 H_{X,h,t}$ ) is then the isotope composition of xylem water at stem base at time  $t - \tau$ .

$$\delta^2 H_{X,h,t} = \delta^2 H_{X,0,t-\tau} \quad (10)$$

where  $\tau$  is the lag before  $\delta^2 H_{X,0,t}$  reaches stem height  $h$  (Fig. 2a), which depends on the true sap flux density in the xylem ( $SF_v$ ). True sap flux density indicates the real speed of vertical water displacement within a plant,

derived by dividing  $SF_t$  over the lumen area of the plant ( $A_x$ ; Fig. 2a) i.e. the total cross-sectional area of the vessels.  $\tau$  can be obtained from the mass conservation equality:

$$h \cdot A_x = \int_{t-\tau}^t SF_t dt \quad (11)$$

Note that since most scientific studies express sap flux density as the sap flow over the total sapwood area ( $SF_S$ ), rather than over the total vessel lumen area ( $SF_V$ ), for consistency, we will present the model outputs as functions of  $SF_S$ .

Note that  $SF_V$  presents the sap flux density normalized over the total vessel lumen area, and as vessel lumen area correlates with plant diameter at breast height (DBH), there is no need for explicit consideration of DBH in the model for comparison among field measurements.

Model analyses show that the impact of the mutual diffusion coefficient of heavy water in normal water on the transport flux is negligible for plants with high sap flux densities, which is the case for the theoretical examples below. However, in plants with low sap flow densities, consideration of diffusion might be required. Diffusion might also be generated by water passing through a complex network of vessels, in analogy to diffusion in a porous media (see supplementary methods B for some analytical results, simulated cases of and a detailed discussion on the role of diffusion). SWIFT was implemented in R version 3.4.0 (R Core Team, 2017), and is publicly available (see GitHub repository HannesDeDeurwaerder/SWIFT).

### iii. Model parameterization and analyses

The model's primary purpose is to gain insight into 1) which processes are capable of generating  $\delta_{\text{xyt}}$  variance, and 2) how sensitive the variance in  $\delta_{\text{xyt}}$  along the stem is in response to the modeled plant hydraulic processes. To this end, we adopted the basic plant parameters from Huang *et al.* (2017) who studied soil-plant hydrodynamics of loblolly pine (*Pinus taeda* L.) during a 30-day extended dry down period (Table S1). We started with synthetic basal sap flow patterns and volumes extracted from the model runs of Huang *et al.* (2017) for a typical drought day (day 11). Both basal sap flow patterns and volumes are repeated over the studied period, as no variation between days is assumed. Sap flow follows the plant's water demand which is the result of daily cycles of transpiration driven by photosynthetic active solar radiation (PAR), vapor pressure deficit (VPD), and optimal stomatal response (Epila *et al.*, 2017). Secondly, both the soil matric potential ( $\Psi_{S,i,t}$ ) and  $\delta^2\text{H}$  composition of soil water ( $\delta^2H_{S,i}$ ) profiles with soil depth were adopted from Meißner *et al.* (2012) (Fig. S8, see Table S1 for equations) as driver data of the model, and were assumed to stay constant over time. Since measurements of Meißner *et al.* (2012) were conducted at a silt loam plot in the temperate climate of central Germany, corresponding soil parameters were selected from Clapp & Hornberger (1978). Subsequently, the following model simulations were executed (see Fig. 2a):

- 1) **Analysis A1: impact of temporal  $SF_t$  variation on the isotope composition of xylem water at a fixed stem height.** Temporal patterns in  $\delta^2\text{H}$  isotope composition in xylem water ( $\delta^2H_X$ ) were evaluated for a typical situation, i.e. measurement at breast height ( $h=1.30$  m) (e.g. White *et al.*, 1985; Meinzer *et al.*, 1999; Goldsmith *et al.*, 2012; Hervé-Fernández *et al.*, 2016; De Deurwaerder *et al.*, 2018; Muñoz-Villers *et al.*, 2019).



- 2) **Analysis A2: impact of temporal  $SF_t$  variation at different tree heights.** Temporal patterns in  $\delta^2H_X$  within a tree at various sampling heights (5, 10, and 15 m).
- 3) **Analysis A3: impact of temporal  $SF_t$  variation on the isotope composition of xylem water and the timing of sampling.** Representation of the profile of  $\delta^2H_X$  along the full height of a tree, measured at different sampling times (9:00 and 11:00), with the standard parameterization given in Table S1.
- 4) **Analysis B: variation in  $\delta^2H_X$  due to differences in absolute daily average sap flow speed.** Diurnal patterns in the  $\delta^2H_X$  in trees that differ solely in daily averaged  $SF_V$ , which are set to 0.64, 0.42, and 0.19 m h<sup>-1</sup>, respectively corresponding to  $SF_S$  values of 0.09, 0.06 and 0.03 m h<sup>-1</sup>.
- All parameters of the four analyses are given in Table S1. The model simulations for each analysis were compared to a null model.

iv. *The null model*

The null model adopts the standard assumption of zero variation in  $\delta_{xyl}$  along the length of the plant body, but allows for potential measurement errors related to the extraction protocol. In reality, empirically obtained data will have some variation as observed values ( $Obs. \delta_{xyl}$ ) are the sum of the true  $\delta_{xyl}$ -values and their extraction error ( $error_{extraction}$ ).

$$Obs. \delta_{xyl} = True \delta_{xyl} + error_{extraction} \quad (12)$$

Hence, the null model attributes any variance in isotopic composition to extraction errors, with maximum extraction error ranges of 3‰ for  $\delta^2H$  samples (0.3‰ for  $\delta^{18}O$ ) expected for water extraction recovery rates higher than 98% (e.g. Orłowski *et al.*, 2013). These extraction errors are negatively skewed following the Rayleigh distillation model, which predicts that extraction error for incomplete water recovery will be negative, and therefore  $Obs. \delta_{xyl} \leq True \delta_{xyl}$ . The null model represents this  $error_{extraction}$  by a negative skew-normal distribution (with location parameter  $\zeta = 0\text{‰}$ , the scale  $\omega = 3\text{‰}$  for  $\delta^2H$  or 0.3‰ for  $\delta^{18}O$ , and shape  $\alpha = -\infty$ ) (Azzalini, 2013).

### 2.2.2. Estimation of average RWU depth

Average RWU depths (i.e. the weighted mean of the depths of RWU, with the uptake fractions at the different depths as weights) were derived from the simulated  $\delta^2H_X$  values by use of both the direct inference method and the end-member mixing analysis method. Together, these techniques represent 96% of the applied methods in the literature (Rothfuss & Javaux, 2017), and the reader is referred to Rothfuss & Javaux (2017) for a complete discussion of both techniques. In line with the general approach assessing RWU with stable water isotopes, the average RWU depth is obtained by relating the  $\delta^2H_X$  with the  $\delta^2H_{S,i}$  depth profile. We compared average RWU depth estimates obtained from simulated  $\delta^2H_X$ , as described in the analyses above, with the true average RWU depth. Here, the true average RWU depth was defined as the depth corresponding to the daily weighted average  $\delta^2H_X$ , calculated as the weighted sum of  $\delta^2H_{X,i,t}$  and the relative fraction of water taken up at each depth.

### 2.2.3. Transport dynamics and sensitivity analysis

We perform a basic model validation of our model assumption that the propagation of an isotopic signature is driven by diurnal sap flow dynamics and diffusion alone. In essence, the model assumes that once water with a given isotopic signature enters the stem, it moves upwards with the speed of sap flow, and changes only due to the effect of diffusion. The effects of capacitance on  $\delta^2H_X$  dynamics by the release of storage water in the xylem flow can be ignored. To validate this assumption we compare model predictions against observed  $\delta^2H_X$  dynamics monitored within a pine tree (*Pinus pinea* L.) following  $^2H$ -enrichment in a controlled greenhouse experiment, as detailed in Marshall *et al.* (2020).  $\delta^2H_X$  was measured at two heights (0.15 and 0.65m) using a novel *in situ* technique, the borehole equilibration method. Performed model simulations consider the absolute ranges of sap flux densities during the entire monitoring campaign, with the account of tree tapering effect on sap flux densities over the studied stem length (supplementary method C). Validation of diurnal variation in  $\delta^2H_X$  requires high temporal resolution monitoring of  $\delta^2H_X$  dynamics in plants stems, with simultaneous high temporal resolution monitoring and characterization of sap flow, soil water potential, and isotopic composition. Such data does not yet exist to our best of knowledge.

In addition, we performed two sensitivity analyses to assess the relative importance of each parameter in generating variance in  $\delta^2H_X$  along the length of a plant. In both sensitivity analyses, we varied model parameters one-at-a-time to assess the local sensitivity of the model outputs for soil type, sap flux density, root properties, and sampling strategies. The sensitivity analysis provides insight into possibilities for improving the design of field protocols, by revealing potential key measurements and caveats in field setups. More details on the performed sensitivity analysis and validation of transport dynamics are available in supplementary method C.

### 3. Results

#### 3.1. Part A: Empirical exploration

The null model assumes constant isotopic composition of root water uptake, with only limited variance in isotopic composition introduced by extraction errors ( $\beta^2H_X < 3\text{‰}$ ;  $\delta^{18}O_X < 0.3\text{‰}$ ). However, pronounced  $\delta^2H_X$  variance within individual plants, exceeding the null model ranges, are observed in all three independent datasets. The normalized  $\delta^2H$  composition in xylem water ( $\beta^2H_X$ ) along the stem length of lianas and trees in French Guiana exceeded the null model by a factor of 3.2 and 4.3, respectively (Fig. 3c, Fig. S2). Differences up to 13.1‰ and 18.3‰ in  $\delta^2H$  and 1.3‰ and 2.2‰ in  $\delta^{18}O$  were observed in individuals of trees and lianas, respectively (Supplementary method A, table A.).

Similarly, diurnal intra-individual  $\delta^2H_X$  variances were found for all considered plant growth forms, i.e. trees, shrubs, and herbs, monitored in China (Fig. 4b-d, Fig S3). Observed daily maximum differences in  $\delta^2H_X$  were 18.0‰, 21.0‰, and 25.2‰ for trees, shrubs and herbs respectively (2.8‰, 6.8‰, and 6.5‰ in  $\delta^{18}O_X$  in Fig. S4). The expected null model variance was exceeded for each species during its measurement period.

Finally, pronounced intra-individual  $\delta^2H_X$  variance was also observed for all monitored firs and beeches in Germany (Fig 4e, Fig. S5). Here, daily maxima differences in  $\delta^2H_X$  were 8.2 ‰ and 14.2 ‰ for *Abies alba* and *Fagus sylvatica* respectively (2.0‰ and 4.2 ‰ in  $\delta^{18}O_X$  in Fig. S6).

### 3.2. Part B: Model exploration

#### *Isotope composition of xylem water at stem base and basic model behavior*

At the stem base, simulated  $\delta^2H_{X,0,t}$  displays a diurnal fluctuation (Fig. 2b, Fig S7) that corresponds to the daily sap flow pattern (Fig. S7). This pattern is caused by shifting diurnal average RWU depth. Early in the morning, when transpiration is low, most of the RWU occurs in deeper layers, where soil matric potential is less negative and where soil water is more depleted in  $^2H$  compared with the soil layers above (Fig. S8a-b). As transpiration increases during the day, a significant proportion of RWU can now be extracted from the drier, shallower layers, where the soil water is enriched in  $^2H$ , i.e., having a higher  $\delta^2H$ . In the afternoon, as transpiration declines, the isotopic composition reflects again the composition of the more depleted soil water in the deeper soil layers, and it remains constant throughout the night because apart from diffusion SWIFT does not consider mixing of the internal stem water. The mixing effects of diffusion are only noticeable at low sap flow speeds (Fig. 3b).

Highest  $\delta^2H_X$ -values (approx. -59‰) are found in alignment with the diurnal minimum of  $\Psi_{X,0,t}$  (approx. -0.85 MPa, Fig. S7). At this moment, the difference between  $\Psi_{X,0,t}$  and  $\Psi_{S,i,t}$  is maximal, enabling water extraction from the upper and driest soil layers. Most root biomass is located near the surface (cf. Jackson *et al.*, 1995; Fig. S8c) and uptake in these layers will result in relatively high contributions to the total RWU.

In contrast, differences between  $\Psi_{X,0,t}$  and  $\Psi_{S,i,t}$  are smaller in the early morning and late afternoon causing root water uptake in the upper soil layers to halt. The decreasing in absolute range of  $\Delta\Psi_{i,t}$  translates into higher proportions of RWU originating from deeper, more depleted soil layers. This causes  $\delta^2H_X$  to drop to a baseline of approx. -67‰. This afternoon depletion of  $\delta^2H_X$  will henceforth be referred to as the  $\delta^2H_X$ -baseline drop.

#### *Isotope composition of xylem water at different times, heights and $SF_V$*

Temporal fluctuation in  $\delta^2H_X$  within a tree at 1.3 m (i.e. the standard sampling height; Analysis A1; Fig. 2a) and other potential sampling heights (e.g. branch collection; Analysis A2; Fig. 2a), are provided in Fig. 2b and 3a. Both analyses show that fluctuations in  $\delta^2H_X$  depend on the height of measurement and the corresponding time needed to move the water along the xylem conduits. Note that it depends on the selected temporal resolution whether the  $\delta^2H_X$ -baseline drop at a given height equals the (stem base) minimum (here 1 min, see Fig. S12). In addition to sampling height, analysis A3 depicts the importance of sampling time (Fig. 3a). Outputs of analysis B predict that the occurrence and width of the  $\delta^2H_X$ -baseline drop are a function of the sap flow velocity  $SF_V$  (Fig. 3b). To aid model interpretation and comparability with field data, we (i) provide an illustrative example of normalized  $\delta^2H$  isotope composition of model-simulated xylem water ( $\beta^2H_X$ ) with consideration of extraction error (Fig. 4a), and (ii) display the relation between  $\delta^2H_X$  variance and cumulative sap flow volumes, for which the piston flow dynamics in SWIFT originate from lateral translation of the  $\delta^2H_X$  fluctuation at  $\delta^2H_{X,0,t}$  (Fig. 2b).

#### 3.2.1. Potential biases in average RWU depth estimation

Both timing of measurement (Fig. 5a) and  $SF_V$  (Fig. 5b) influence average RWU depth estimates derived via the direct inference and end-member mixing analysis method (Fig. S9). Collection of tree samples at 1.30 m can result in erroneous estimation, deviating up to 104 % from the average daily RWU depth (Fig. 5). Plotting the relative

error in average RWU depth as a function of time and  $SF_V$  (Fig. 5) shows that it is possible to time  $\delta^2H_X$  measurements in a fashion that captures unbiased estimates of the average RWU depth. Xylem water sampling should be timed to capture the  $\delta^2H_X$  that corresponds to water extracted at peak RWU, and the expected sampling time can be derived by considering the time needed for the water to reach the point of measurement (i.e. at 1.30 m in Fig. 5).

### 3.2.2. Transport dynamics and sensitivity analysis

Our sensitivity analyses show that the expected absolute error in average RWU depth assessment is directly related to both 1) maximum variance in and 2) the probability of sampling non-representative  $\delta^2H_X$  values. The maximum variance depends on the height, while the probability of sampling non-representative areas depends on the width of the “ $\delta^2H_X$ -baseline drop” respectively (defined above). Hence, variation in  $\delta^2H_X$  is determined by several factors, including the sampling strategy (timing and height of sampling), sap flow velocity (Fig. S10), and below-ground biophysical parameter (Fig. S11). We summarized the most important variables as predicted by SWIFT, which should be considered in subsequent RWU studies.

Plants on loamy soils show larger diurnal  $\delta^2H_X$  variances in comparison with those on clay soils for a similar prevailing isotope gradient across the soil profile. Larger variances correspond to potentially larger errors, but the steeper slope of the  $\delta^2H_X$  curve results in a thinner  $\delta^2H_X$ -baseline drop. Hence, loamy soil can result in potentially the large error but this is mediated by a lower probability of sampling non-representative  $\delta^2H_X$  values during the day.

The volume of water taken up by the plant ( $SF_t$ ; Fig. S11b) affects xylem water potential of the plant at stem base ( $\hat{\Psi}_{X,0,t}$ ). Higher  $SF_t$  requires more negative  $\hat{\Psi}_{X,0,t}$ , enabling the plant to access the enriched soil water of more shallow soil layers. Therefore, an increase in  $SF_t$  results in the increase of maximum  $\delta^2H_X$  values (increased maximum error) but also results in a smaller width of the baseline drop (Fig. 2-3). Lower  $SF_t$  result in smaller errors, but a larger probability of sampling a non-representative area (Fig. 3b).

Root properties, i.e. root membrane permeability (Fig. S11c) strongly influence both the total range of  $\delta^2H_X$  variance and the width of the  $\delta^2H_X$ -baseline drops. Decreasing root membrane permeability, but with no alterations to the sap flow volumes, results in thinner  $\delta^2H_X$ -baseline drops, but higher maximum  $\delta^2H_X$  variance.

In addition, the true sap flow velocity ( $SF_t$  per unit of lumen area) will determine the relative importance of diffusion on the  $\delta^2H_X$  dynamics. Diffusion can cause a smoothing of the peak and a consequent increase in the width of the  $\delta^2H_X$ -baseline drop. However, as diffusion is proportional to the time that water isotopologues remain in the xylem, its absolute impact on  $\delta^2H_X$  is negligible in plants with a high true sap flow velocity. In contrast, the impact of diffusion on  $\delta^2H_X$  dynamics is substantial for plants with very low velocities, where water takes many days to pass from roots to leaves (see supplementary method B).

The role of diffusion was investigated using a stepwise  $^2H$  enrichment experiment in Marshall *et al.* (2020) (Fig 6). Analytical solutions of an advection-diffusion equation show that at 0.15 cm, a relatively small diffusivity was required to reproduce the initial increase of xylem isotope signature, with values comparable to these reported for diffusivity of heavy water (Meng *et al.*, 2018). However, at 65 cm, the value of diffusivity required to match the observed initial increase was much higher, suggesting other

processes besides molecular diffusivity might contribute to the isotope transport (e.g. variable flow velocities within vessels and among vessels of the xylem network). Note also that the analytical solutions were not able to recover the second part of the curve where the isotope reaches the asymptotic enriched value, which is more gradual in the observations (Fig. 6). This also suggests a complex transport of  $\delta^2H_X$  in the xylem.

## 4. Discussion

### 4.1. Dynamic diurnal isotope compositions of xylem water along plant stems

Empirical field data show pronounced  $\delta_{xyl}$  variance along the stem length (Fig. 3) and over a sub-daily time period (Fig. 4). Our model explorations suggest that basic plant hydraulic functioning can result in shifting mixtures of  $\delta^2H_X$  entering the plant (Fig. 2-3). Daily  $\Psi_{x,0,t}$  fluctuations interact with the  $\Psi_{s,i,t}$  profile causing different parts of the root distribution to be active during the day. The fluctuations in  $\delta^2H_X$  at the stem base propagate along the xylem with a velocity proportional to the sap flow and this produces variability in sampled  $\delta^2H_X$  that is much larger than the expected measuring error. Consequently, rather than being static,  $\delta^2H_X$  values along the height of a plant should be envisioned as a dynamic diurnal process.

Importantly, we show that high variance in  $\delta^2H_X$  can result in an incorrect assessment of differences in average RWU depths between plants. Differences do not necessarily result from variability in average RWU depth, but may result from monitoring plants at different heights (Fig. 2-3), at different times (Fig. 3a) or by comparing individuals which have different  $SF_V$  (Fig. 3b) and xylem anatomical properties. For example, depending on  $SF_V$  and lumen area, the isotopic signal can take hours or days to travel from roots to leaves - as was also observed experimentally (Steppe *et al.*, 2010; Magh *et al.*, 2020; Marshall *et al.*, 2020).

Low  $SF_V$  allows multiple  $\delta^2H_X$ -baseline drops over the length of a single tree. Sampled  $\delta^2H_X$  can reflect soil isotopic composition of the past several days. Our sensitivity analysis reveals that various soil and plant characteristics have an important role in determining both the daily maximum  $\delta^2H_X$  variance as well as the width of the  $\delta^2H_X$  - baseline drop. These two characteristics directly impact (i) the expected maximum bias in estimates of average RWU depth and (ii) the chance of measuring  $\delta^2H_X$  values that do not represent a mixture of all rooting layers during peak RWU (i.e. measurements in the baseline drop). Ultimately, these factors will challenge the use of stable water isotope to study the terrestrial water fluxes as recently reviewed by Penna *et al.* (2018). We additionally advocate that future research should explore the minimum set of (bio)physiological drivers and processes that require quantification to correctly interpret  $\delta^2H_X$  along the hydraulic pathway length of a plant.

### 4.2. General applicability of model and results

A necessary condition for diurnal shifts in RWU is the existence of water potential differences, e.g. more negative water potentials in the upper layers where trees usually have higher root density, which can cause a disproportional partitioning of diurnal RWU between deep and shallow roots over a diurnal course. The pronounced variance in  $\delta_{xyl}$  identified in this study is intrinsic to the isotopic tracing technique for RWU assessment, as this method relies on the existence of a soil water isotopic profile. Such profiles are the result of soil evaporation, a process inextricably coupled to water potential heterogeneity, and hence to variance in  $\delta^2H_X$ .

Plant transpiration results from a complex interaction between atmospheric demands (i.e. driven by VPD and radiation) and stomatal conductance that depends on tolerance for drought stress and soil moisture content. We may expect diurnal fluctuation in radiation and VPD, and hence in water transport and depth of water absorption, as modeled here to be a general phenomenon in nature. Moreover, much greater fluctuations in VPD and radiation should be expected under natural conditions than the diurnal cycle described here, and these will increase the variability of transpiration fluxes, leading to even more complex dynamics of  $\Psi_{x,0,t}$ . Specifically, the model simulations suggest that intra-individual variability of  $\delta^2H_x$  will reflect the past changes of RWU dynamics, including RWU dynamics driven by changes of environmental demands. For instance, a changing degree in cloud cover that impacts sap flow dynamics can influence  $\Psi_{x,0,t}$  rather abruptly (e.g. in lianas; Chen *et al.*, 2015) and lead to instantaneous changes in the  $\delta^2H$  composition of the water mixture taken up at the root level. This can complicate the comparison of different plants sampled at different heights and times.

Note that, based on our model, we expect that soil isotopic enrichment experiments will generate extensive  $\delta^2H_x$  variation along the length of trees whenever diurnal RWU fluctuations cause water extraction to shift between labeled and unlabeled soil layers. Furthermore, when enrichment experiments target trees with different hydraulic properties (such as  $SF_v$ ) care should be taken to determine when and where to sample these trees to assess a potential  $^2H$  enrichment in xylem water (Fig. 6, but see Magh *et al.*, 2020;).

### 4.3. Alternative causes of $\delta_{xyl}$ fluctuation

The SWIFT model provides a simple traceable and mechanistic explanation, using diurnal variations in  $SF_t$  and RWU, for the pronounced variance and dynamic nature of the  $\delta_{xyl}$  fluctuations with plant height and time of field samples (e.g. Fig. 3-4) and elsewhere (Cooper *et al.* 1991). However, several other processes might contribute to generate variability, while others can act to damp this variability. In the next section, we will discuss alternative causes, complementary and antagonistic, that contribute to the observed intra-individual  $\delta_{xyl}$  variances.

#### i. Fractionation at root or stem level

An increasing body of observations shows the occurrence of isotopic fractionation at the root level governed by root membrane transport (Lin & Sternberg, 1993; Vargas *et al.*, 2017) or by unknown reasons (Zhao *et al.*, 2016). Brinkmann *et al.* (2019) hypothesize that root level fractionation causes disparity when average RWU depth calculations based on  $\delta^2H_x$  measurements are compared with those of  $\delta^{18}O_x$ . However, it is difficult to imagine a scenario where root fractionation by itself can explain the observed diurnal fluctuations in  $\delta_{xyl}$  with height and time. Even if root fractionation significantly contributed to variation in  $\delta_{xyl}$ , we would still need to take into account diurnal fluctuation in RWU to explain the observed patterns. Isotopic enrichment of xylem water along the stem length was observed in association with stem transpiration (Dawson & Ehleringer, 1993; Barnard *et al.*, 2006). However, this phenomenon is generally restricted to non-suberized plants and in woody branches in close vicinity to the evaporative surface of the plant (Dawson & Ehleringer, 1993). Isotopic enrichment can, therefore, not explain the variances in  $\delta_{xyl}$  observed in our empirical data, which were sampled within the main stem (data French Guiana) or from lignified branch segment distant from evaporative surfaces (data China and Germany).

#### ii. Temporal and spatial soil dynamics

Soil water content can be extremely heterogeneous in the three spatial dimensions as well as in time with complex dynamics of soil water movement. For example, hydraulic lift vertically redistributes soil water through the roots (Dawson & Ehleringer, 1993), which may change the water isotopic composition of the water mixture in the rhizosphere that is taken up by roots. Specifically, hydraulic lift redistributes and mixes the isotopic signal of depleted soil water in deeper layers with the enriched soil water signal in the rhizosphere in shallower layers. This should lead to lower variation in the soil water accessible to the plant, and hence less variation along plant height. Horizontal heterogeneity of water content may also affect  $\delta_{xyl}$  variance as soil water potentials and the isotope composition of soil water are interlinked. Under these conditions, it is important to understand how much the radial distribution of roots will naturally average out soil heterogeneity. However, note that heterogeneity in the soil does not automatically translate in variability in the xylem. Differential root water uptake driven by the diurnal fluctuation in water potential gradients in the soil-plant interface is still required to generate variability in the xylem isotopic signature.

### iii. *Storage tissue and phloem enrichment*

Storage tissues release water and sugars into the xylem conduits on a daily basis to support water transpiration demand (Goldstein et al., 1998; Morris et al., 2016; Secchi et al., 2017) or to repair embolism (Salleo et al., 2009; Secchi et al., 2017). Both water and sugars are transported in and out of storage tissue via symplastic pathways using plasmodesmata and aquaporins (Knipfer et al., 2016; Secchi et al., 2017), a pathway that has been linked to isotopic fractionation in roots (Ellsworth & Williams, 2007). Moreover, phloem transports photosynthetic assimilates that were produced in the leaves and are therefore potentially affected by transpiration fractionation (Gessler et al., 2013). Hence, these metabolic molecules might show higher values of  $\delta^2H$  and  $\delta^{18}O$  compared to RWU. Water release from storage or phloem tissue might locally alter  $\delta_{xyl}$  (White et al., 1985). Additionally, the time between water storage and release could bridge multiple days, and corresponding isotopic composition may reflect soil conditions antecedent a dry spell when the isotopic signature of soil was less vertically stratified. It is evident that such dynamics are complex, and it is hard to predict how storage tissue and phloem enrichment affect observed  $\delta_{xyl}$  patterns. Importantly, xylem isotopic sampling cannot differentiate between water resulting from RWU or storage, and therefore we cannot exclude the possibility that tissue and phloem enrichment play a role. At a minimum this adds further uncertainty to RWU assessment. Water derived from storage tissues might also be present in larger fraction in higher parts of the plants, especially branches, as contamination accumulates as water moves upwards.

Unfortunately, to our best knowledge, empirical data on the isotopic composition of storage tissue and its spatiotemporal dynamics are absent in the literature. Future research should target impact assessment of storage water on intra-individual  $\delta_{xyl}$ , allowing proper implementation in the model.

### iv. *Diffusion processes*

Diffusion is a process of net movement of molecules from a region of higher concentration to a region of lower concentration. Consequently, diffusion dampens  $\delta_{xyl}$  variability, both in time and space within water xylem. Although the mutual diffusion coefficient of heavy water in normal water is very small and flow within vessels is laminar, other processes might still contribute to generating diffusion along the xylem. For example, as the water moves through the complex network of vessels, differences in velocities between vessels of different sizes cause

some particles to move faster or slower than average flow. According to the Hagen–Poiseuille law, the flow in each vessel is proportional to the fourth power of the vessel radius and the mean velocity to the square of the radius, thus potentially generating large differences in particle velocities depending on the vessel size distribution and other anatomical properties. Even within a single vessel, velocity is parabolic with a maximum flow velocity in the center and zero at the vessel walls.

#### 4.4. A way forward

The observed large  $\delta_{xyl}$  variance and temporal dynamics in the empirical data suggest the need for a critical assessment of the stable isotope tracer technique for RWU studies. However, it also creates new opportunities. Since  $\delta_{xyl}$  variance and temporal dynamics herein likely relate to various plant physiological processes, monitoring of variation in  $\delta_{xyl}$  can allow a more integrated understanding of plant water transport and hydraulic properties.

Combining a plant hydraulic model with *in situ*  $SF_v$ ,  $\delta^2H_{s,i}$  and  $\Psi_{s,i,t}$  can also help improve the robustness of RWU assessment and interpretation. Measurements of  $\delta^2H_{s,i}$  and  $\Psi_{s,i,t}$  at multiple depths, i.e. by installing soil water suction cups working at a vacuum (i.e. Rennenberg *et al.*, 1996) and multiple soil matric potential sensors that measure at a high temporal frequency, should be especially valuable since the SWIFT model showed high sensitivity to alterations of this variable and these can be directly supplied as model inputs. At the same time, the availability of  $SF_i$  measurements allows for identifying the moment when water uptake from all root layers is at its maximum, which can be used to determine the optimal timing of sampling at a given height providing a more robust estimation of average RWU depth and uptake.

Alongside the modeling approach presented here, new ways to study  $\delta^2H_x$  at a high temporal scale are strongly encouraged. For example, the pioneering work of Volkmann *et al.* (2016) to the development of an *in situ* continuous isotope measurement technique that offers the possibility for monitoring  $\delta_{xyl}$  at a sub-hourly resolution. This technique holds strong promise for further elucidating the natural  $\delta^2H_x$  variances found within plants and the physiology processes from which these variances result. Such high temporal resolution of isotope measurements, coupled with *in situ* monitoring of various environmental and plant biophysical metrics, are needed for both model improvement and further validation. Moreover, these seem inevitable to eventually differentiate all causal mechanisms of the observed intra-individual  $\delta_{xyl}$  variance.

#### 5. Conclusions

A collection of empirical field data show pronounced variance and high temporal fluctuations in  $\delta_{xyl}$ . Moreover, these high temporal fluctuations in  $\delta_{xyl}$  emanate from basic plant hydraulic functioning as model explorations show. We expect the observed  $\delta_{xyl}$  variance and sub-daily fluctuations result, for a large part, from the mechanisms considered here, though various other physiological processes could also affect  $\delta_{xyl}$ .

Our theoretical explorations warn that variability in the isotope composition of plant xylem water can result in erroneous average RWU depth estimation and will complicate the interpretation and comparison of data: samples taken at different heights, times or plants differing in  $SF_v$  may incorrectly show differences in average RWU depth. We further predict that various soil parameters and plant hydraulic parameters affect (i) the absolute size of the error and (ii) the probability of measuring  $\delta_{xyl}$  values that do not represent the well-mixed values during the plants' peak RWU. Hydraulic models, such as SWIFT, could help to design more robust sampling regimes that enable



improved comparisons between studied plants. We advocate the addition of  $SF_t$ , which indirectly reflects diurnal RWU fluctuations, and  $\Psi_{s,i,t}$  monitoring as a minimum in future RWU assessments since these parameters were predicted to be the predominant factors introducing variance in  $\delta_{xyl}$  from the SWIFT model exploration. However, soil texture and root permeability are also key measurements especially when comparing across species and sites.

Our findings do not exclude additional factors that impact the observed intra-individual  $\delta_{xyl}$  variance and temporal fluctuation as many processes can act simultaneously and are not mutually exclusive. Therefore, we strongly emphasize the need for more research. Directed studies that validate and quantify the relative impact of other plant physiological processes towards variance in  $\delta_{xyl}$  are a prerequisite before improved modeling tools can be developed.

## Acknowledgment

This research was funded by the European Research Council Starting Grant 637643 (TREECLIMBERS), the FWO grants (1507818N, V401018N to HDD), the Carbon Mitigation Initiative at Princeton University (MD, MDV), Agence Nationale de la Recherche “Investissement d’Avenir” grant (CEBA: ANR-10-LABX-25-01), the Belgian American Educational Foundation (BAEF to FM) and the WBI (FM). LW acknowledges partial support from the Division of Earth Sciences of National Science Foundation (EAR-1554894). We are grateful to Samuel Bodé, Megan Bartlett, Isabel Martinez Cano, and Pedro Hervé-Fernández who provided feedback on analytical and interpretative aspects of the study. We thank Dries Van Der Heyden, Wim Van Nunen, Laurence Stalmans, Oscar Vercleyen, Katja Van Nieuland, Stijn Vandevoorde, and Clément Stahl for data collection and lab processing. We credit Pascal Petronelli and Bruce Hoffman for species identification, and Cora N. Betsinger for proofreading. Cheng-Wei Huang’s work provided inspiration for this research.

## Author contribution

H.V., M.D.V, and P.B. supervised and provided guidance throughout all aspects of the research. H.D.D., M.D.V, and H.V. designed the study. H.D.D., K.K., R.K.M., J.D.M., L.W., and L.Z. collected and processed the empirical datasets. The model was developed and coded by H.D.D, M.D.V, M.D., and F.M. All authors contributed to the interpretation of the results and the text of the manuscript.

## Data availability

Both the French Guiana data and the SWIFT model are available on the GitHub repository HannesDeDeurwaerder/SWIFT. For the availability of the data collected in China and Germany, readers are referred to Zhao *et al.* (2014) and Magh *et al.* (2020), respectively.

## Competing interests

The authors declare that they have no conflict of interest.

## References

- Araguás-Araguás L, Froehlich K, Rozanski K. 1998.** Stable isotope composition of precipitation over southeast Asia. *Journal of Geophysical Research: Atmospheres* **103**: 28721–28742.
- Azzalini A. 2013.** *The skew-normal and related families*. Cambridge University Press.
- Barbeta A, Gimeno TE, Clavé L, Fréjaville B, Jones SP, Delvigne C, Wingate L, Ogée J. 2020.** An explanation for the isotopic offset between soil and stem water in a temperate tree species. *New Phytologist*.
- Barnard RL, De Bello F, Gilgen AK, Buchmann N. 2006.** The  $\delta^{18}\text{O}$  of root crown water best reflects source water  $\delta^{18}\text{O}$  in different types of herbaceous species, *Rapid Commun. Mass Sp.*, 20, 3799–3802.
- Brinkmann N, Eugster W, Buchmann N, Kahmen A. 2019.** Species-specific differences in water uptake depth of mature temperate trees vary with water availability in the soil. *Plant Biology* **21**: 71–81.
- Čermák J, Ulrich R, Staněk Z, Koller J, Aubrecht L. 2006.** Electrical measurement of tree root absorbing surfaces by the earth impedance method: 2. Verification based on allometric relationships and root severing experiments. *Tree physiology* **26**: 1113–1121.
- Cernusak LA, Farquhar GD, Pate JS. 2005.** Environmental and physiological controls over oxygen and carbon isotope composition of Tasmanian blue gum, *Eucalyptus globulus*. *Tree physiology* **25**: 129–146.
- Chen Y, Cao K, Schnitzer SA, Fan Z, Zhang J, Bongers F, Chen Y. 2015.** Water-use advantage for lianas over trees in tropical seasonal forests. : 128–136.
- Clapp RB, Hornberger GM. 1978.** Empirical equations for some soil hydraulic properties. *Water resources research* **14**: 601–604.
- Cooper LW, DeNiro MJ, Keeley JE. 1991.** The relationship between stable oxygen and hydrogen isotope ratios of water in astomatal plants.
- Dawson TE, Ehleringer JR. 1991.** Streamside trees that do not use stream water. *Nature* **350**: 335–337.
- Dawson TE, Ehleringer JR. 1993.** Isotopic enrichment of water in the “woody” tissues of plants: implications for plant water source, water uptake, and other studies which use the stable isotopic composition of cellulose. *Geochimica et Cosmochimica Acta* **57**: 3487–3492.
- Dawson TE, Mambelli S, Plamboeck AH, Templer PH, Tu KP. 2002.** Stable isotopes in plant ecology. *Annual review of ecology and systematics* **33**: 507–559.
- De Deurwaerder H, Hervé-Fernández P, Stahl C, Burban B, Petronelli P, Hoffman B, Bonal D, Boeckx P, Verbeeck H. 2018.** Liana and tree below-ground water competition—evidence for water resource partitioning during the dry season. *Tree Physiology*.
- Doussan C, Pierret A, Garrigues E, Pagès L. 2006.** Water uptake by plant roots: II—modelling of water transfer in the soil root-system with explicit account of flow within the root system—comparison with experiments. *Plant and soil* **283**: 99–117.

629 **Ehleringer JR, Dawson TE. 1992.** Water uptake by plants: perspectives from stable isotope composition. *Plant,*  
630 *Cell & Environment* **15**: 1073–1082.

631 **Ellsworth PZ, Williams DG. 2007.** Hydrogen isotope fractionation during water uptake by woody xerophytes.  
632 *Plant and Soil* **291**: 93–107.

633 **Epila J, Maes WH, Verbeeck H, Camp J Van, Okullo JBL, Steppe K. 2017.** Plant measurements on African  
634 tropical *Maesopsis eminii* seedlings contradict pioneering water use behaviour. *Environmental and Experimental*  
635 *Botany* **135**: 27–37.

636 **Früh T, Kurth W. 1999.** The hydraulic system of trees: theoretical framework and numerical simulation.  
637 *Journal of theoretical Biology* **201**: 251–270.

638 **Gessler A, Brandes E, Keitel C, Boda S, Kayler ZE, Granier A, Barbour M, Farquhar GD, Treydte K.**  
639 **2013.** The oxygen isotope enrichment of leaf-exported assimilates—does it always reflect lamina leaf water  
640 enrichment? *New Phytologist* **200**: 144–157.

641 **Goldsmith GR, Muñoz-Villers LE, Holwerda F, McDonnell JJ, Asbjornsen H, Dawson TE. 2012.** Stable  
642 isotopes reveal linkages among ecohydrological processes in a seasonally dry tropical montane cloud forest.  
643 *Ecohydrology* **5**: 779–790.

644 **Goldstein G, Andrade JL, Meinzer FC, Holbrook NM, Cavelier J, Jackson P, Celis A. 1998.** Stem water  
645 storage and diurnal patterns of water use in tropical forest canopy trees. *Plant, Cell & Environment* **21**: 397–406.

646 **Hervé-Fernández P, Oyarzún C, Brumbt C, Huygens D, Bodé S, Verhoest NEC, Boeckx P. 2016.** Assessing  
647 the ‘two water worlds’ hypothesis and water sources for native and exotic evergreen species in south-central  
648 Chile. *Hydrological Processes* **30**: 4227–4241.

649 **Huang C, Domec J, Ward EJ, Duman T, Manoli G, Parolari AJ, Katul GG. 2017.** The effect of plant water  
650 storage on water fluxes within the coupled soil–plant system. *New Phytologist* **213**: 1093–1106.

651 **Jackson PC, Cavelier J, Goldstein G, Meinzer FC, Holbrook NM. 1995.** Partitioning of water-resources  
652 among plants of a lowland tropical forest. *Oecologia* **101**: 197–203.

653 **De Jong van Lier Q, Van Dam JC, Metselaar K, De Jong R, Duijnisveld WHM. 2008.** Macroscopic root  
654 water uptake distribution using a matric flux potential approach. *Vadose Zone Journal* **7**: 1065–1078.

655 **Knipfer T, Cuneo I, Brodersen C, McElrone AJ. 2016.** In-situ visualization of the dynamics in xylem  
656 embolism formation and removal in the absence of root pressure: a study on excised grapevine stems. *Plant*  
657 *Physiology*: pp-00136.

658 **Lanning M, Wang L, Benson M, Zhang Q, Novick KA. 2020.** Canopy isotopic investigation reveals different  
659 water uptake dynamics of maples and oaks. *Phytochemistry* **175**: 112389.

660 **Lin G, Sternberg L. 1993.** Hydrogen isotopic fractionation by plant roots during water uptake in coastal  
661 wetland plants. Stable isotopes and plant carbon-water relations. Elsevier, 497–510.

662 **Magh R-K, Eiferle C, Burzlaff T, Dannenmann M, Rennenberg H, Dubbert M. 2020.** Competition for water

rather than facilitation in mixed beech-fir forests after drying-wetting cycle. *Journal of Hydrology*: 124944.

**Mamonov AB, Coalson RD, Zeidel ML, Mathai JC. 2007.** Water and deuterium oxide permeability through aquaporin 1: MD predictions and experimental verification. *The Journal of general physiology* **130**: 111–116.

**Marshall JD, Cuntz M, Beyer M, Dubbert M, Kuehnhammer K. 2020.** Borehole equilibration: testing a new method to monitor the isotopic composition of tree xylem water in situ. *Frontiers in Plant Science* **11**: 358.

**Meinzer FC, Andrade JL, Goldstein G, Holbrook NM, Cavelier J, Wright SJ. 1999.** Partitioning of soil water among canopy trees in a seasonally dry tropical forest. *Oecologia* **121**: 293–301.

**Meißner M, Köhler M, Schwendenmann L, Hölscher D. 2012.** Partitioning of soil water among canopy trees during a soil desiccation period in a temperate mixed forest. *Biogeosciences* **9**: 3465–3474.

**Meng W, Xia Y, Chen Y, Pu X. 2018.** Measuring the mutual diffusion coefficient of heavy water in normal water using a double liquid-core cylindrical lens. *Scientific reports* **8**: 1–7.

**Meunier F, Rothfuss Y, Bariac T, Biron P, Richard P, Durand J-L, Couvreur V, Vanderborght J, Javaux M. 2017.** Measuring and modeling hydraulic lift of *Lolium multiflorum* using stable water isotopes. *Vadose Zone Journal*.

**Morris H, Plavcová L, Cvecko P, Fichtler E, Gillingham MAF, Martínez-Cabrera HI, McGlinn DJ, Wheeler E, Zheng J, Ziemińska K. 2016.** A global analysis of parenchyma tissue fractions in secondary xylem of seed plants. *New Phytologist* **209**: 1553–1565.

**Muñoz-Villers LE, Geris J, Alvarado-Barrientos S, Holwerda F, Dawson TE. 2019.** Coffee and shade trees show complementary use of soil water in a traditional agroforestry ecosystem. *Hydrology and Earth System Sciences Discussion*.

**Orlowski N, Frede HG, Brüggemann N, Breuer L. 2013.** Validation and application of a cryogenic vacuum extraction system for soil and plant water extraction for isotope analysis. *J. Sens. Sens. Syst* **2**: 179–193.

**Penna D, Hopp L, Scandellari F, Allen ST, Benettin P, Beyer M, Geris J, Klaus J, Marshall JD, Schwendenmann L. 2018.** Ideas and perspectives: Tracing terrestrial ecosystem water fluxes using hydrogen and oxygen stable isotopes—challenges and opportunities from an interdisciplinary perspective. *Biogeosciences*.

**Phillips DL, Gregg JW. 2003.** Source partitioning using stable isotopes: coping with too many sources. *Oecologia* **136**: 261–269.

**Rennenberg H, Schneider S, Weber P. 1996.** Analysis of uptake and allocation of nitrogen and sulphur compounds by trees in the field. *Journal of Experimental Botany* **47**: 1491–1498.

**Rothfuss Y, Javaux M. 2017.** Reviews and syntheses: Isotopic approaches to quantify root water uptake: a review and comparison of methods. *Biogeosciences* **14**: 2199.

**Salleo S, Trifilò P, Esposito S, Nardini A, Gullo MA Lo. 2009.** Starch-to-sugar conversion in wood parenchyma of field-growing *Laurus nobilis* plants: a component of the signal pathway for embolism repair? *Functional Plant Biology* **36**: 815–825.

697 **Scholander PF. 1966.** The role of solvent pressure in osmotic systems. *Proceedings of the National Academy of*  
698 *Sciences of the United States of America* **55**: 1407.

699 **Secchi F, Pagliarani C, Zwieniecki MA. 2017.** The functional role of xylem parenchyma cells and aquaporins  
700 during recovery from severe water stress. *Plant, cell & environment* **40**: 858–871.

701 **Steppe K, Lemeur R. 2004.** An experimental system for analysis of the dynamic sap-flow characteristics in  
702 young trees: results of a beech tree. *Functional Plant Biology* **31**: 83–92.

703 **Steppe K, De Pauw DJW, Doody TM, Teskey RO. 2010.** A comparison of sap flux density using thermal  
704 dissipation, heat pulse velocity and heat field deformation methods. *Agricultural and Forest Meteorology* **150**:  
705 1046–1056.

706 **Vargas AI, Schaffer B, Yuhong L, Sternberg L da SL. 2017.** Testing plant use of mobile vs immobile soil  
707 water sources using stable isotope experiments. *New Phytologist* **215**: 582–594.

708 **Vogel T, Dohnal M, Dusek J, Votrubova J, Tesar M. 2013.** Macroscopic modeling of plant water uptake in a  
709 forest stand involving root-mediated soil water redistribution. *Vadose Zone Journal* **12**.

710 **Volkman THM, Kühnhammer K, Herbstritt B, Gessler A, Weiler M. 2016.** A method for in situ  
711 monitoring of the isotope composition of tree xylem water using laser spectroscopy. *Plant, cell & environment*  
712 **39**: 2055–2063.

713 **Walker CD, Richardson SB. 1991.** The use of stable isotopes of water in characterizing the source of water in  
714 vegetation. *Chemical Geology* **94**: 145–158.

715 **Wershaw RL, Friedman I, Heller SJ, Frank PA. 1966.** Hydrogen isotopic fractionation of water passing  
716 through trees. *Advances in organic geochemistry*: 55.

717 **White JWC, Cook ER, Lawrence JR, Broecker WS. 1985.** The D/H ratios of sap in trees - implications for  
718 water sources and tree-ring D/H ratios. *Geochimica et Cosmochimica Acta* **49**: 237–246.

719 **De Wispelaere L, Bodé S, Hervé-Fernández P, Hemp A, Verschuren D, Boeckx P. 2016.** Plant water  
720 resource partitioning and xylem-leaf deuterium enrichment in a seasonally dry tropical climate. *Biogeosciences*  
721 *Discuss.* **2016**: 1–26.

722 **Yakir D. 1992.** Variations in the natural abundance of oxygen-18 and deuterium in plant carbohydrates. *Plant,*  
723 *Cell & Environment* **15**: 1005–1020.

724 **Yang Q, Xiao H, Zhao L, Zhou M, Li C, Cao S. 2010.** Stable isotope techniques in plant water sources: a  
725 review. *Sciences in Cold and Arid Regions* **2**: 112–122.

726 **Zhao L, Wang L, Cernusak LA, Liu X, Xiao H, Zhou M, Zhang S. 2016.** Significant difference in hydrogen  
727 isotope composition between xylem and tissue water in *Populus euphratica*. *Plant, Cell & Environment* **39**:  
728 1848–1857.

729 **Zhao L, Wang L, Liu X, Xiao H, Ruan Y, Zhou M. 2014.** The patterns and implications of diurnal variations  
730 in the d-excess of plant water, shallow soil water and air moisture. *Hydrol. Earth Syst. Sci.* **18**: 4129–4151.

731 **Zhao L, Xiao H, Zhou J, Wang L, Cheng G, Zhou M, Yin L, McCabe MF. 2011.** Detailed assessment of  
732 isotope ratio infrared spectroscopy and isotope ratio mass spectrometry for the stable isotope analysis of plant  
733 and soil waters. *Rapid Communications in Mass Spectrometry* **25**: 3071–3082.

734 **Zimmermann U, Ehhalt D, Münnich K. 1967.** Soil-Water movement and evapotranspiration: changes in the  
735 isotopic composition of the water. Conference on Isotopes in Hydrology. Vienna, 567-585.

736

Symbol	Description	Unit
$A_{R,i}$	The absorptive root area distribution over soil layer $i$	$\text{m}^2$
$A_{Rtot}$	The plants' total active fine root surface area	$\text{m}^2$
$A_{\text{SAPWOOD}}$	Sapwood area	$\text{m}^2$
$A_x$	Total lumen area	$\text{m}^2$
$b$	Shape parameter for the soil hydraulic properties (Clapp & Hornberger, 1978)	dimensionless
$B_i$	The overall root length density distribution per unit of soil, not necessarily limited to the focal plant.	$\text{m m}^{-3}$
$\delta^2H_{X,0,t}$	Isotope composition of plant xylem water at stem base at time $t$	in ‰ VSMOW
$\delta^2H_{X,h,t}$	Isotope composition of plant xylem water at height $h$ and time $t$	in ‰ VSMOW
$\delta^2H_{S,i}$	Isotope composition of soil water of the $i^{\text{th}}$ soil layer (constant over time)	in ‰ VSMOW
$\delta_{\text{sample}}$	Isotope composition of water within a sample	in ‰ VSMOW
$\Delta\Phi_{i,t}$	Estimated water potential gradient between stem base and the $i^{\text{th}}$ soil layer at time $t$ derived from Eq. (8)	$\text{m}$
$\Delta\Psi_{i,t}$	Soil matric potential gradient between soil and roots at the $i^{\text{th}}$ soil layer at time $t$	$\text{m H}_2\text{O}$
$\beta^2H_X; \beta^{18}O_X$	Normalized isotope composition of plant xylem water	in ‰ VSMOW
$f_{i,t}$	The fraction of water taken up in the $i^{\text{th}}$ soil layer at time $t$	dimensionless
$h$	Measurement height	$\text{m}$
$i$	Soil layer index	dimensionless
$\delta_{\text{xyl}}$	Isotope composition of plant xylem water	in ‰ VSMOW
$k_i$	Soil-root conductance of the $i^{\text{th}}$ soil layer	$\text{s}^{-1}$
$K_{\text{max}}$	Maximum soil hydraulic conductivity	$\text{m s}^{-1}$
$k_R$	Effective root radial conductivity	$\text{s}^{-1}$
$k_S$	The conductance associated with the radial water flow between the soil and the root surface	$\text{s}^{-1}$
$K_{S,i}$	Soil hydraulic conductivity at the $i^{\text{th}}$ soil layer	$\text{m s}^{-1}$
$\ell$	The approximated radial pathway length of water flow between bulk soil and root surface	$\text{m}$
LF	Lumen fraction per unit sapwood area	$\text{m}^2 \text{m}^{-2}$
$n$	Number of unique contributing water sources	#
$\Psi_{\text{sat}}$	Soil matric potential at soil saturation	$\text{m}$
$\Psi_{S,i,t}$	Soil matric potential of the $i^{\text{th}}$ soil layer at time $t$	$\text{m}$
$\Psi_{X,0,t}$	Water potential at the base of the plant stem at time $t$	$\text{m}$
$R$	Heavy to light isotope ratio measured in the sample or standard	‰
$RWU_{i,t}$	Net amount of water entering and leaving the root tissues per unit of time in the $i^{\text{th}}$ soil layer at time $t$	$\text{m}^3 \text{s}^{-1}$

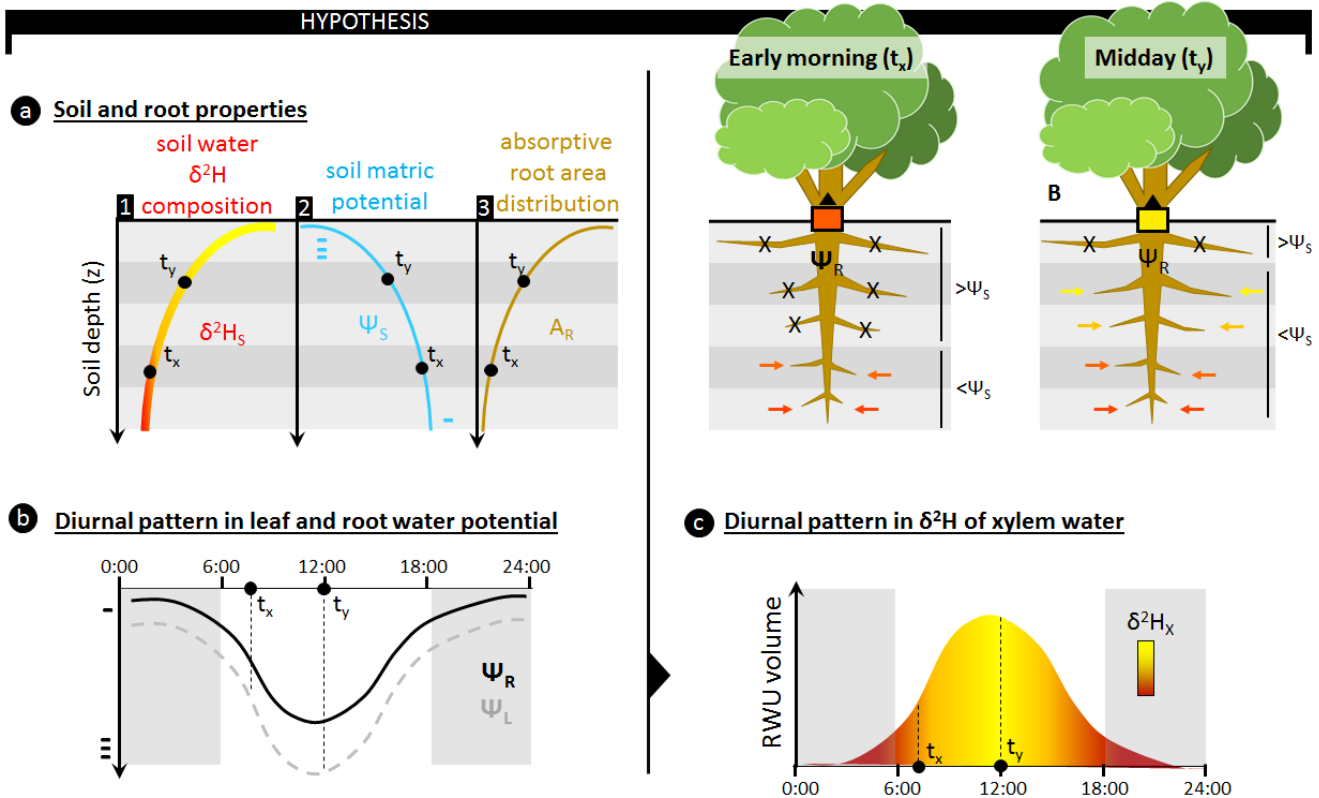
$SF_t$	Instantaneous sap flow at time $t$	$\text{m}^3 \text{ s}^{-1}$
$SF_S$	Sap flow velocity, calculated as the sap flow per sapwood area	$\text{m h}^{-1}$
$SF_V$	True sap flux density, calculated as the sap flow per lumen area	$\text{m h}^{-1}$
$\tau$	Delay before the isotope composition of xylem water at stem base reaches stem height $h$	s
$\theta_{sat}$	Soil moisture content at soil saturation	$\text{m}^3 \text{ m}^{-3}$
$\theta_{S,i,t}$	Soil moisture content of the $i^{\text{th}}$ soil layer at time $t$	$\text{m}^3 \text{ m}^{-3}$
$z_i$	Soil depth of the $i^{\text{th}}$ soil layer	m

---

739

740

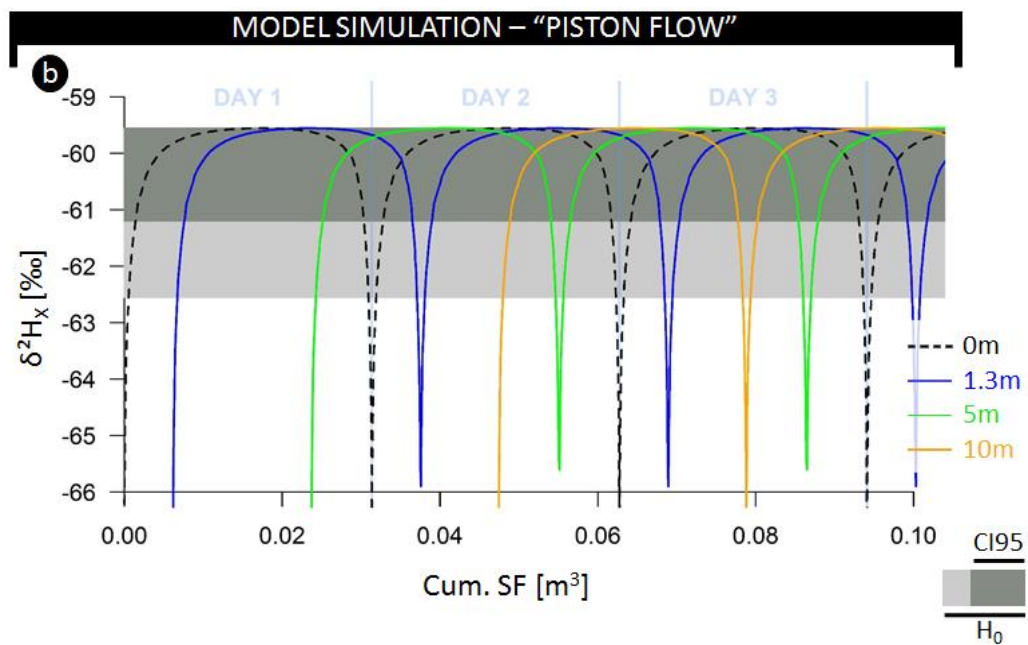
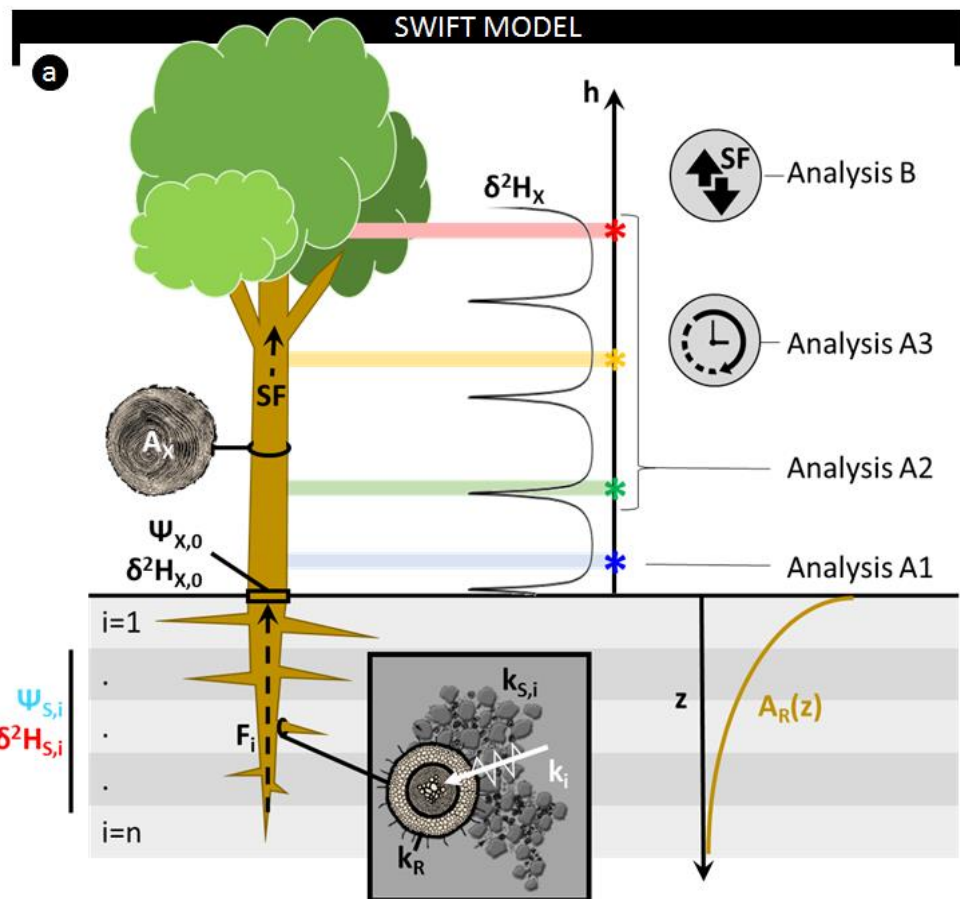




742

**Fig 1.** The use of stable water isotopes ( $\delta^2\text{H}$  and  $\delta^{18}\text{O}$ ) to assess the relative depth of root water uptake (RWU) requires a depth gradient in isotopic composition of soil water ( $\delta^2\text{H}_s$ ) to be present (**a, line 1**), as only then can the relative contribution of different soil layers to the isotopic composition in a plant's xylem water ( $\delta^2\text{H}_X$ ) be derived. These  $\delta^2\text{H}_s$  gradients occur naturally as the result of evaporative soil drying during drought conditions, however, these conditions also result in the formation of a gradient in soil matric potential ( $\Psi_s$ ), ensuring an increasing  $\Psi_s$  with depth (**a, line 2**). RWU and sap flow in plants are passive processes where water flows in the direction of decreasing water potentials. Specifically for RWU, this implies that water influx through the absorptive root area ( $A_R$ ; **a, line 3**) of a plant's root is facilitated whenever the water potential in the root ( $\Psi_R$ ) is more negative than the surrounding  $\Psi_s$ . As  $A_R$  and  $\Psi_s$  are generally not uniform with soil depth (z), the relative contribution of a specific soil layer to RWU will depend on (i) the difference between  $\Psi_s$  and  $\Psi_R$  in that soil layer, and (ii) the relative amount of absorptive root area in that soil layer. Stable water isotopes techniques assume that the  $\delta^2\text{H}_X$  reflects the contribution of  $\delta^2\text{H}_s$  from all soil layers. However, this does not account for diurnal fluctuations in  $\Psi_R$  which are invoked by the diurnal patterns in a plant's transpiratory water demands (**panel b**). Typically, more negative  $\Psi_R$  values are observed when water demands are high, i.e. around midday. However, a decrease in  $\Psi_R$  will result in higher RWU, and alter the contribution of different soil layers to RWU. Specifically, dryer and shallower soil layers, with more negative  $\Psi_s$ , could start contributing to RWU as  $\Psi_R$  decreases (**panel c**). For example, in the early morning (situation  $t_x$ ) when  $\Psi_R$  is high, only deeper soil layers where  $\Psi_s > \Psi_R$  contribute to overall  $\delta^2\text{H}$  composition of the RWU flux. As  $\Psi_L$  and  $\Psi_R$  decrease towards midday (situation  $t_y$ ) more water can be absorbed from shallower soil layers. As the  $A_R$  in these shallow soil layers is high, they strongly affect the relative

762 contribution of  $\delta^2H_S$  entering the plant. Hence, diurnal fluctuations in  $\Psi_R$  will result in fluctuating mixtures of  $\delta^2H_S$   
763 entering the plant. As these  $\delta^2H_S$  mixtures are transported along the xylem pathway, they produce variance in  $\delta^2H_X$ ,  
764 which could complicate RWU assessments via stable water isotope analysis.



765

766

**Fig. 2. (a)** Schematic representation of the model and considered analysis detailed in the text. **(b)** Simulated fluctuations in  $\delta^2H$  composition of plant xylem water as a function of the cumulative sap flow volume measured at various heights: stem base (0 m, black dashed), 1.3 m (blue), 5 m (green) and 10 m (red). The horizontal grey colored envelope delineates the acceptable variance from the stem mean according to the null model ( $H_0$ ), i.e. assuming no variance along the length of a lignified plant aside from potential extraction error (i.e. 3‰). Herein, the dark grey envelope indicates the confidence interval comprising 95% of potential extraction error (CI95).

774

775

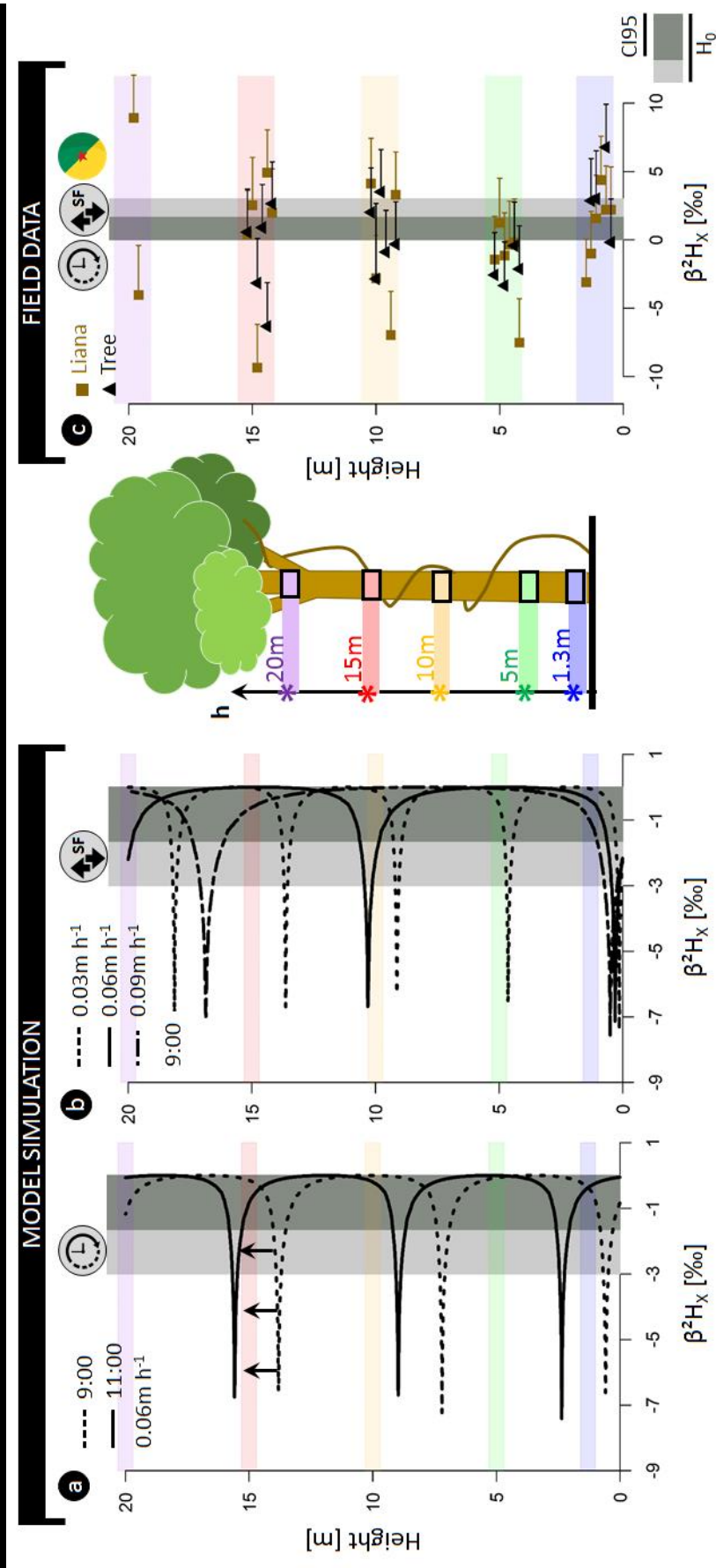


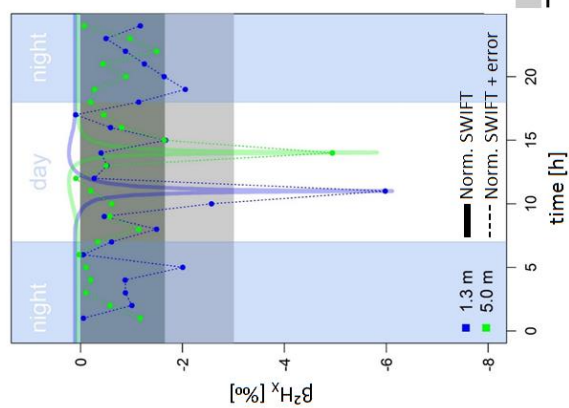
**Fig 3. (a)** Model outputs for model analysis A3 representing the normalized  $\delta^2\text{H}$  composition of xylem water ( $\beta^2\text{H}_\text{X}$ ) as a function of the tree height simulated for different sampling times (9:00 and 11:00). The modeled tree has an average daily sap flux density of  $0.06 \text{ m h}^{-1}$  ( $SF_\text{S}$ ;  $\sim$  daily true sap flux density  $SF_\text{V} = 0.42 \text{ m h}^{-1}$ ). **(b)** Model outputs for model analysis B where  $\beta^2\text{H}_\text{X}$  in relation to stem height is shown at 9:00 a.m., but parameterized with distinct  $SF_\text{S}$ , i.e.  $0.09$ ,  $0.06$  and  $0.03 \text{ m h}^{-1}$  (corresponding to  $SF_\text{V}$  of  $0.64$ ,  $0.42$  and  $0.19 \text{ m h}^{-1}$ , respectively). The standard parameterization used for both study analysis is detailed in Table S1. **(c)** Field measurements of  $\beta^2\text{H}_\text{X}$  for six lianas (■) and six trees (▲). Error whiskers are the combination of potential extraction and measurement errors of the isotope analyzer. A species-specific breakdown of the field data is provided in Fig S2. The horizontal grey colored envelope in all panels delineates the acceptable variance from the stem mean according to the null model ( $H_0$ ), i.e. assuming no variance along the length of a lignified plant aside from potential extraction error (i.e. 3‰). Herein, the dark grey envelope indicates the confidence interval comprising 95% of potential extraction error (CI95).

## NORMALIZATION AND ERROR

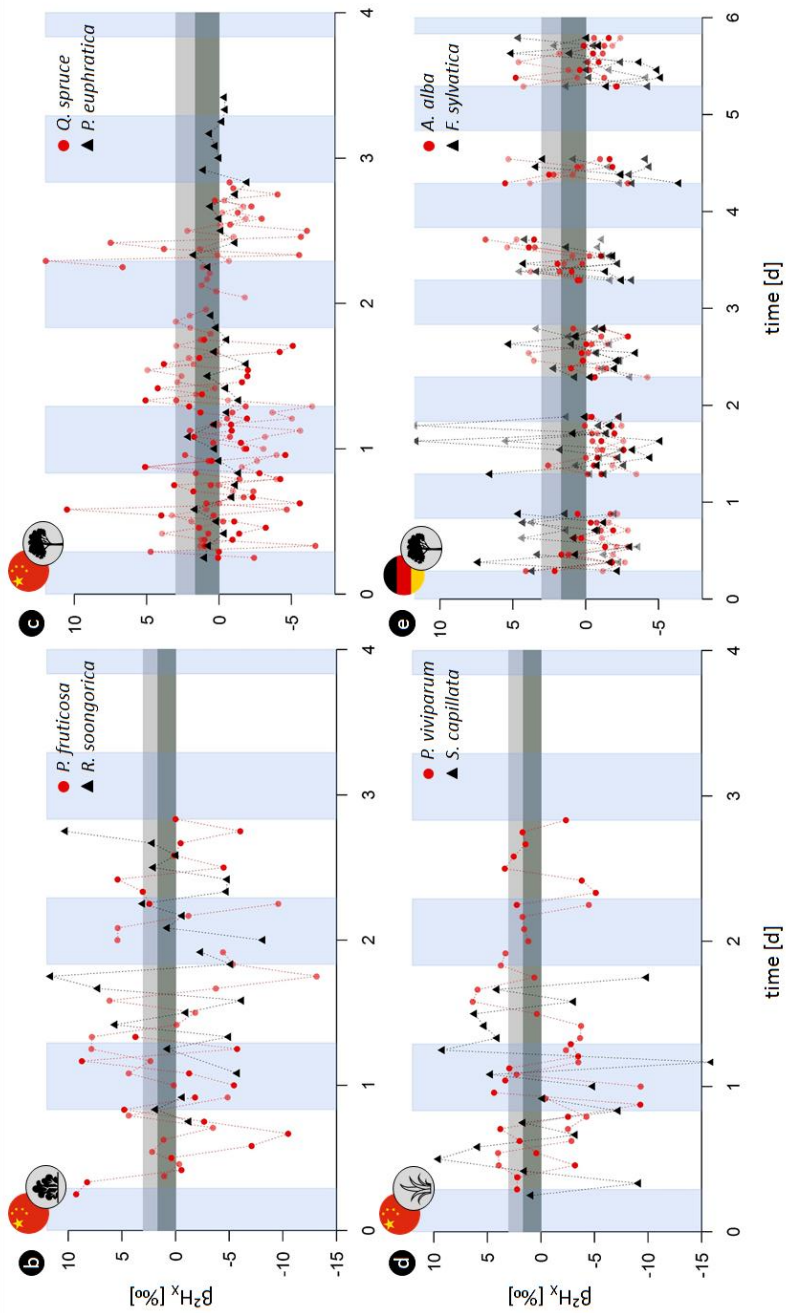
$$\beta^2 H_X = \delta^2 H_X - \frac{1}{N} \sum_{j=1}^N \delta^2 H_{Xj}$$

$N$  = number of sampled heights or timesteps during one day

$Error \sim SN(\xi = 0\%; \omega = 3\%; \alpha = -\infty)$

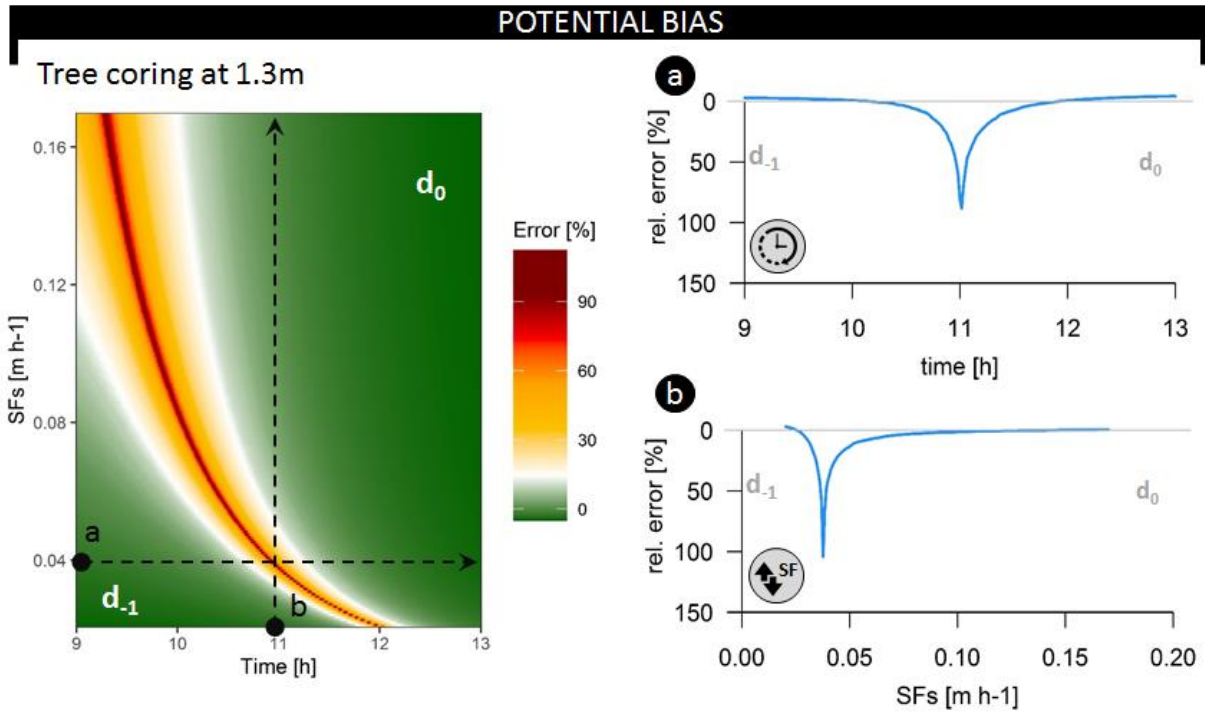


## TEMPORAL FIELD DATA



**Fig 4. (a)** Illustrative example of model simulations transformed in normalized  $\delta^2\text{H}$  composition of xylem water ( $\beta^2\text{H}_\text{X}$ ) at 1.3 (blue) and 5m (green) sampling height, with the formula provided. Thicker lines indicate model simulations without error, line connected dots indicate a scenario of hourly sampling with consideration of extraction error (i.e. a negative skew-normal distribution;  $\zeta = 0\text{‰}$ , the scale  $\omega = 3\text{‰}$ , and shape  $\alpha = -\infty$ ). **(b-e)** High temporal field measurements of  $\beta^2\text{H}_\text{X}$  of (b) two shrubs, (c) two trees, and (d) two herb species sampled in the Heihe River Basin (northwestern China); and (e) two tree species sampled in the “Freiamt” field site in south-west Germany. The horizontal grey colored envelope in all panels delineates the acceptable variance from the stem mean according to the null model ( $H_0$ ), i.e. assuming no variance along the length of a lignified plant aside from potential extraction error (i.e. 3‰). Herein, the dark grey envelope indicates the confidence interval comprising 95% of potential extraction error (CI95). A breakdown of the field data on species and individual level is provided in the supplementary figures (Fig S3-S4-S5-S6)





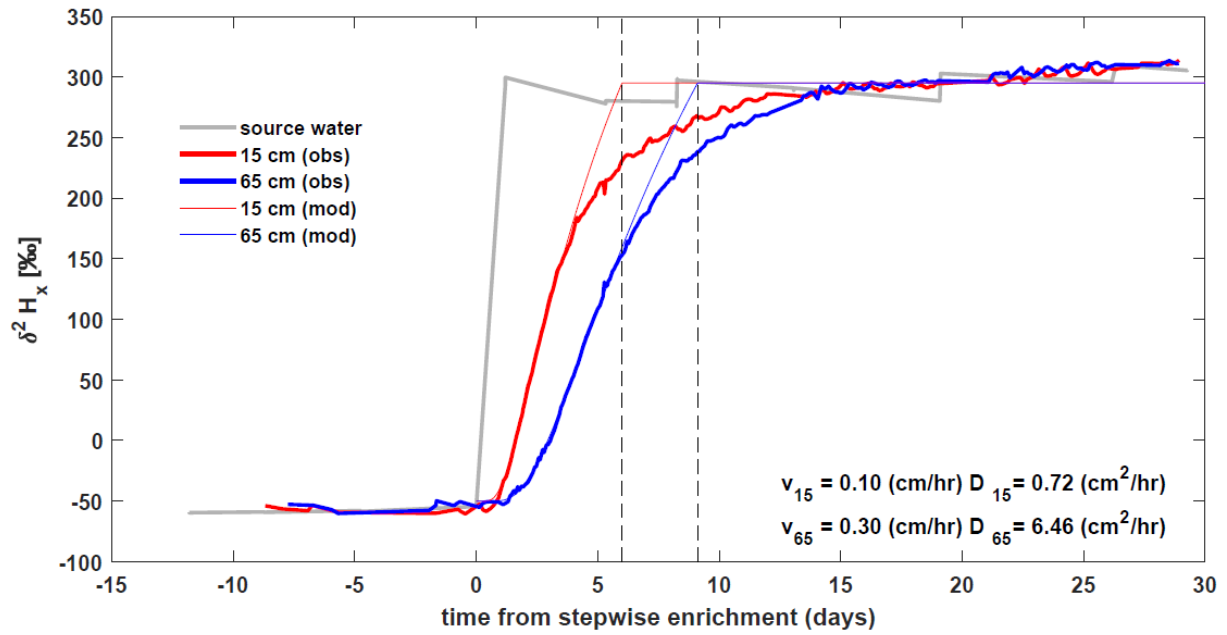


**Fig. 6.** Basic model validation, comparing continuous *in situ*  $\delta^2H_x$  measurements of a stepwise  $^2H$  enrichment experiment (Marshall *et al.*, 2020) with analytical solutions of advection-diffusion equation, at heights 0.15m (—) and 0.65m (—) on a pine tree (*Pinus pinea* L). The source water of the intact-root, isotopic enrichment greenhouse experiment, is presented in grey. Model parameters, velocity, and diffusion were fitted by visual inspection independently for the two heights to match the initial increase in isotope signature (values reported in the bottom right)